

Signaling Between TRPV1/TRPV4 and Intracellular Hydrostatic Pressure in the Mouse Lens

Nicholas A. Delamere,¹ Mohammad Shahidullah,¹ Richard T. Mathias,² Junyuan Gao,² Xiuron Sun,² Caterina Sellitto,² and Thomas W. White²

¹Department of Physiology, University of Arizona, Tucson, Arizona, United States

²Department of Physiology & Biophysics, Stony Brook University, Stony Brook, New York, United States

Correspondence: Thomas W. White, BST 5-147, School of Medicine, Stony Brook, NY 11794-8661, USA; thomas.white@stonybrook.edu.

Received: April 15, 2020

Accepted: May 20, 2020

Published: June 29, 2020

Citation: Delamere NA, Shahidullah M, Mathias RT, et al. Signaling between TRPV1/TRPV4 and intracellular hydrostatic pressure in the mouse lens. *Invest Ophthalmol Vis Sci.* 2020;61(6):58.

<https://doi.org/10.1167/iovs.61.6.58>

PURPOSE. The lens uses feedback to maintain zero pressure in its surface cells. Positive pressures are detected by transient receptor potential vanilloid (TRPV4), which initiates a cascade that reduces surface cell osmolarity. The first step is opening of gap junction hemichannels. One purpose of the current study was to identify the connexin(s) in the hemichannels. Negative pressures are detected by TRPV1, which initiates a cascade that increases surface osmolarity. The increase in osmolarity was initially reported to be through inhibition of Na/K ATPase activity, but a recent study reported it was through stimulation of Na/K/2Cl (NKCC) cotransport. A second purpose of this study was to reconcile these two reports.

METHODS. Intracellular hydrostatic pressures were measured using a microelectrode/manometer system. Lenses from TRPV1 or Cx50 null mice were studied. Specific inhibitors of Cx50 gap junction channels, NKCC, and Akt were used.

RESULTS. Either knockout of Cx50 or blockade of Cx50 channels completely eliminated the response to positive surface pressures. Knockout of Cx50 also caused a positive drift in surface pressure. The short-term (~20-minute) response to negative surface pressures was eliminated by blockade of NKCC, but a long-term (~4-hour) response restored pressure to zero. Both short- and long-term responses were eliminated by knockout of TRPV1 or inhibition of Akt.

CONCLUSIONS. Hemichannels made from Cx50 are required for the response to positive surface pressures. Negative surface pressures first activate NKCC, but a backup system is inhibition of Na/K ATPase activity. Both responses are initiated by TRPV1 and go through PI3K/Akt before branching.

Keywords: Cx50, TRPV1, TRPV4, Na/K ATPase, Na/K/2Cl cotransporter, intracellular pressure

The anterior surface of the lens is a single layer of cuboidal epithelial cells (E), shown in red in Figure 1A. The basolateral membranes face outward and express the majority of the lens's Na/K ATPase (reviewed in Delamere and Tamiya¹), with activity concentrated at the equator.^{2,3} They also express the majority of lens potassium channels. The cells are coupled together by gap junctions made from Cx43 and Cx50, and they are coupled to underlying fiber cells primarily in the equatorial region.⁴⁻⁷ At the equator, epithelial cells elongate and begin the transformation into fiber cells. The differentiating fibers domain (DF), shown in green in Figure 1A, has a different complement of membrane and cytosolic proteins than its epithelial progenitors. They express large amounts of crystallins in the cytosol, they lose Na/K ATPase activity in the membranes,⁸ and the abundance of potassium channels diminishes while expression of sodium and chloride leak channels increases.⁹⁻¹¹ These fibers are coupled by gap junctions made from Cx50 and Cx46.¹² Their coupling conductance is concentrated in the equatorial region.¹³ Around 15% of the distance

into a lens, fibers lose their internal organelles, membrane proteins undergo significant cleavage, and differentiating fibers become mature fibers. The mature fiber domain (MF) is shown in blue in Figure 1. There is a reduction in gap junction coupling conductance in the MF relative to the DF.¹⁴ The reduction may be due to cleavage of the C-termini from Cx46 and Cx50 at the transition, resulting in a reduction in the open probability of Cx50 channels.¹⁵ Mature fibers, which make up the bulk of the lens, have no organelles or blood vessels, as these would scatter light.¹⁶ They are unable to synthesize new proteins and cannot divide, and yet they are able to survive for the lifetime of the animal. A major factor in the survival of lens fibers is the existence of an internal circulation of ions and water that flows between and through the fibers in very specific manner. The overall pattern of flow is shown superimposed on the sketch of the lens in Figure 1A. Salt and water enter the lens at both poles and exit at the equator. If one looks in more detail (Fig. 1B), the circulation is established by the Na/K ATPase in the epithelium. Because lens cells are extensively coupled

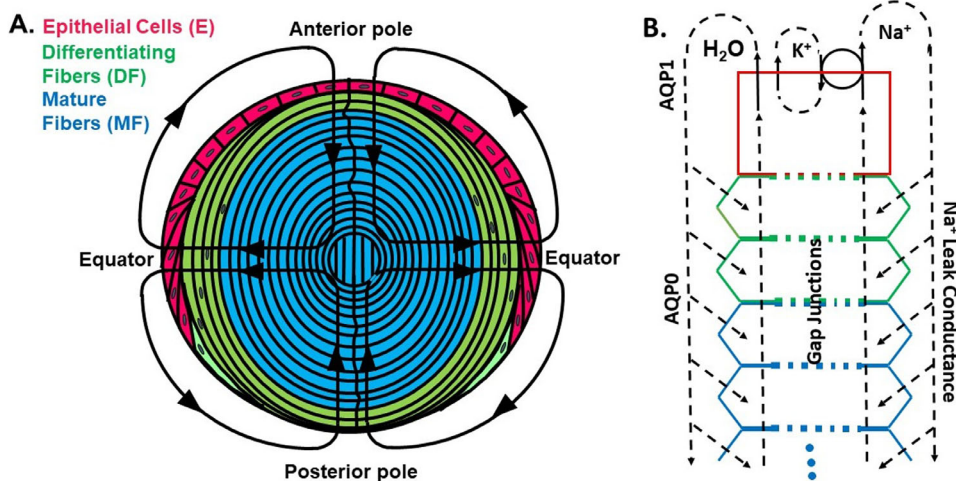


FIGURE 1. The lens circulation. (A) The structure of the lens with the overall pattern of the circulation superimposed in black arrows. (B) A diagram of the radial distribution of the main transporters that generate the circulation.

by gap junctions, the Na/K ATPase is able to generate low intracellular sodium and a negative resting voltage in all lens cells. Sodium flows into the lens through the extracellular spaces between cells, and then it is driven by its transmembrane electrochemical potential to enter fiber cells through membrane sodium leak channels. Once in the fiber cells, it reverses direction and flows to the surface through gap junction channels, which direct the flow toward the equator,¹⁷ where Na/K pump activity is concentrated to transport it out of the lens.^{18,19} The transmembrane movement of sodium creates small osmotic gradients that cause water to follow and circulate in the same pattern.^{3,20,21} The flow of water acts like an internal microcirculatory system, which delivers nutrients and antioxidants to mature fibers (reviewed in Mathias et al.¹³).

The outflow of water along the intracellular pathway is associated with an intracellular hydrostatic pressure gradient. The hydrostatic pressure is highest at the lens center, and its magnitude has been found to vary inversely with the number of open gap junction channels between fibers.³ The pattern of hydrostatic pressure appears to be similar in different species of lens,²² and the magnitude increases somewhat with age as the number of gap junction channels decreases.²³ In all of the above studies, the intracellular pressure in surface cells of the lens was zero. In other words, at steady state, there is no pressure gradient between the interior of the surface lens cell and extracellular solution. However, when the phosphatase for PI3K, PTEN, was conditionally knocked out in mouse lenses, the lenses began to swell and eventually burst after approximately 12 weeks of age.²⁴ When intracellular hydrostatic pressure was recorded in these lenses, the surface cell pressure increased with age and reached approximately 50 mm Hg at 10 weeks of age. The increase in surface cell pressure was traced to inhibition of the Na/K ATPase. The findings led to the hypothesis that hydrostatic pressure in the lens is regulated by a feedback mechanism that maintains it at zero, and knockout of PTEN interrupts the feedback.

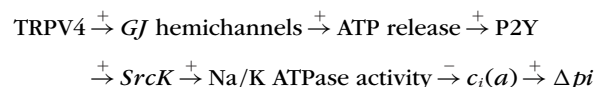
Further studies on the feedback control system for surface cell pressure led to the conclusion there were two feedback paths,²⁵ one that responded to positive changes in surface pressure and the other that responded to negative

changes. Fluid flowing out of the lens across surface cell membranes is driven by a combination of hydrostatic and osmotic pressure.

$$u_m = L_m (\Delta p_i - RT (c_i(a) - c_o)),$$

where u_m (cm/s) is the fluid flow velocity, L_m ((cm/s)/mm Hg) is the membrane hydraulic conductivity, Δp_i is the surface intracellular hydrostatic pressure (mm Hg), $RT = 18.6$ mm Hg/mM at 20°C, $c_i(a)$ (mM) is the total intracellular solute concentration that defines osmolarity at the surface ($r = a$), and c_o is the total solute concentration that defines osmolarity of the solution outside of the lens. Each arm of the feedback mechanism is able to sense Δp_i and make an adjustment to $c_i(a)$ that returns Δp_i to zero, presumably without altering u_m .

Shahidullah et al.^{26,27} showed that hypo-osmotic activation of transient receptor potential vanilloid (TRPV4) initiated the signal transduction cascade shown below. Gao et al.²⁵ showed that this signaling path ultimately regulated positive surface cell pressures back to 0 mm Hg. The pathway elucidated by Shahidullah et al., with the last step determined by Gao et al., is

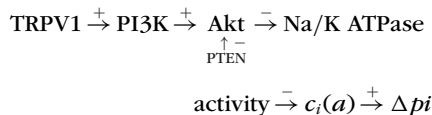


A positive sign means the change in the downstream event goes in the same direction as the upstream change, whereas a negative sign means they go in opposite directions. Thus, an increase in TRPV4 activity ultimately causes a decrease in Δp_i .

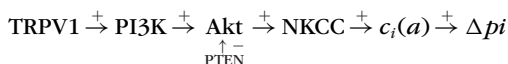
The studies on porcine lens^{26,27} suggested that opening of hemichannels allowed adenosine triphosphate (ATP) release. They were not able to identify the hemichannels and suggested there could be a role for connexins as well as pannexin 1. The lens epithelium expresses gap junction channels made from Cx43 and Cx50. Porcine lens epithelium also expresses pannexin 1.^{26,27} The peripheral fiber cells express gap junctions formed by Cx46 and Cx50 (reviewed

in Mathias et al.¹³). Lens Cx43 forms few if any hemichannels,^{28–30} whereas both Cx46 and Cx50 are robust formers of hemichannels.³¹ One purpose of the current study was to identify the contribution of Cx50 to the lens response to TRPV4 activation.

As regards to the TRPV1-mediated lens response, we initially reported that negative surface pressures were sensed by TRPV1, which then initiated a chain of events (below) that led to partial inhibition of Na/K ATPase activity, which increased surface cell osmolarity and pressure²⁵:



This scheme explained observations in the lens of PTEN knockout (KO) mice. In those lenses, PI3K-mediated phosphorylation of Akt was constitutively active, leading to a chronic decrease in Na/K ATPase activity²⁴, which increased $c_i(a)$ and Δp_i until the capsule ruptured. However, when Shahidullah et al.³² investigated the effect of TRPV1 activation in porcine lenses, they did not find TRPV1-dependent Na/K ATPase inhibition. Instead, they found TRPV1-dependent Na/K/2Cl (NKCC) activation. In a subsequent study,³³ they used TRPV1 KO mice to confirm the role of NKCC activation rather than Na/K pump inhibition as the effector step of the feedback response to negative changes in Δp_i induced by either TRPV4 activation or hyperosmotic solution. This modified scheme is summarized below:



Accordingly, a second purpose of the current study was to reconcile these two different hypotheses and provide one unified hypothesis that explained both studies.

METHODS

Mice were used in accordance with the ARVO statement on the Use of Animals in Ophthalmic and Vision Research. Approximately 2-month-old male mice (C57 BL/6 genetic background) were sacrificed by peritoneal injection of pentobarbital (100 mg/kg of weight). The eyes were removed and placed in a petri dish containing normal Tyrode solution (in mM): NaCl 137.7, NaOH 2.3, KCl 5.4, CaCl₂ 2, MgCl₂ 1, HEPES 5, and Glucose 10, pH 7.4. The cornea and iris were removed and the optic nerve was cut. The sclera was cut into four flaps from the posterior surface and pinned to a sylgard lined chamber, where the experimental protocol was implemented. All experiments were conducted on freshly dissected lenses. TRPV1 KO mice (B6.129X1-Trpv1<tm1Jul>/J) and wild type (WT) of the corresponding C57 genetic background were obtained from the Jackson Laboratory (Ellsworth, ME). Cx50 KO mice³⁴ in the C57 background were obtained from our local colony. The data were analyzed by curve fitting with structurally based models (Equations 1 and 2), using software in Sigma Plot (Systat Software, Inc., San Jose, CA).

Intracellular Hydrostatic Pressures

Intracellular hydrostatic pressures were measured as described in Gao et al.³ For each experiment, an intracellular microelectrode was filled with 3 M KCl solution. The microelectrode was mounted in a patch-clamp pipette holder with a side port. The side port was connected through a plastic tube to a manometer that could both apply and record pressure. Injection of current pulses showed the initial microelectrode resistances in the Tyrode solution bathing the lens were 1.5 to 2 MΩ. The microelectrode was inserted into the lens at 45° between the posterior pole and the equator, and its resistance was again measured. As it was advanced along its 45° track toward the center of the lens, intracellular pressure increased and pushed cytoplasm into the microelectrode tip, causing its resistance to increase. Pressure was applied manually, by adjusting the height of the manometer, to push out the cytoplasm and restore the electrode resistance to its initial value. This entailed up and down adjustment of pressure until we were confident we were applying the minimum pressure necessary to restore the resistance. The value of pressure was then read from a linear scale on the manometer (mm Hg) and entered into the log book along with the distance of the microelectrode tip from the center of the lens (r cm). Pressure could be measured at five or six depths into any one lens, and then data from six to eight lenses of each type were pooled. After completion of the study of each lens, the resistance of the microelectrode was remeasured in the bath. If the resistance had changed, due to either blockage or breakage of the electrode tip, the data were not used. Data from lenses of the same type were pooled and curve fit with Equation 1 to obtain the values of $p_i(r)$ at the lens center ($r = 0$), at the differentiating to mature fiber (DF to MF) transition ($r = b$), and at the lens surface ($r = a$). The value of radius a (cm) was measured in each lens, and then the radial locations were normalized to the radius. The pooled pressure data were graphed and analyzed relative to their fractional distance from the lens center (r/a). The radial location of the DF to MF transition b (cm) was assumed to be given by $b = 0.85a$.

$$p_i(r) = \begin{cases} p_i(a) + (p_i(b) - p_i(a)) \left(\frac{a^2 - r^2}{a^2 - b^2} \right) & b \leq r \leq a \\ p_i(b) + (p_i(0) - p_i(b)) \left(\frac{b^2 - r^2}{b^2} \right) & 0 \leq r \leq b \end{cases} \quad (1)$$

The quadratic r -dependence of pressure suggests the transmembrane entry of water into fiber cells is essentially uniform with depth into the lens.³ The change in slope of the r -dependence at $r = b$ is thought to occur because the number of open-gap junction channels goes down in the MF relative to the DF,¹⁵ and thus the hydraulic conductivity of the DF is higher than that of the MF. The value of $r = 0.85a$ has been used in many past studies of lenses from mice and several other species and always provided a good fit to the data. Moreover, it correlates well with the location of organelle degradation and gap junction protein cleavage (the DF to MF transition). We believe this transition causes a reduction in the number of open-gap junction channels.

The lens is contained in a tough collagenous capsule that prevents placing a microelectrode into a surface cell. When the microelectrode pops through the capsule, it generally lands 10 to 15 cell layers into the lens. However, the surface cell pressure (Δp_i) can be accurately estimated by fitting Equation 1 to pressure data at various depths into the lens and projecting the model to $r = a$. In normal WT lenses,

the projection always gives $p_i(a) = 0$. That is, the best-fit projected pressure at the surface was always 10^{-8} to 10^{-9} mm Hg, which is well beyond our resolution. However, in Cx50 KO lenses, the surface cell pressure is not zero, and the above method was used to estimate its value.

We were also interested in acute changes in surface cell pressure induced by pharmacologic interventions. The microelectrode popped into the lens in a cell near the surface where we measured the pressure ($p_i(r)$ $b < r < a$) for approximately 20 minutes. The time average of the initial pressure was subtracted from the data to give a starting baseline of 0 mm Hg. The change in surface cell pressure Δp caused by a test solution should be similar in any of the cells near the surface (see Equation 1), and the results are presented as the deviation in pressure from the baseline 0 mm Hg. The deviation in pressure from zero in five lenses subjected to the same treatment was averaged to obtain time records.

Fiber Cell Gap Junction Coupling

Impedance was measured as described in Mathias et al.¹⁴ Briefly, the intact lens was pinned to the bottom of a sylgard-lined chamber. A current passing intracellular microelectrode entered the lens at an angle of 45°, at a location halfway between the posterior pole and equator. It was advanced along its track to a central fiber cell, where a stochastic current composed of sinusoidal frequencies between 0 Hz and 5 KHz was injected. On the opposite side of the lens, a second intracellular microelectrode was placed in the lens at 45°, also at a location halfway between the posterior pole and equator. It recorded the induced voltage at various depths from the lens surface. Both signals were sent to a fast Fourier analyzer (Hewlett Packard, Palo Alto, CA), where the intracellular impedance was calculated in real time.

The series resistance ($R_s(r)$ Ω) is the high-frequency asymptote of the magnitude of the lens input impedance. At high frequencies, the impedance of membranes becomes negligible and the lens behaves like a spherical conductor with a point source of current at its center and its surface at ground potential. This model¹⁴ was used to analyze R_s data and is the basis for the following equation:

$$R_s(r) = \begin{cases} \frac{R_{DF}}{4\pi} \left(\frac{1}{r} - \frac{1}{a} \right) & b \leq r \leq a \\ \frac{R_{DF}}{4\pi} \left(\frac{1}{b} - \frac{1}{a} \right) + \frac{R_{MF}}{4\pi} \left(\frac{1}{r} - \frac{1}{b} \right) & 0 \leq r \leq b \end{cases} \quad (2)$$

The radial distance from the lens center is r (cm), the lens radius is a (cm), and the transition from DF to MF occurs at $r = b$ (cm), where experience suggests $b = 0.85a$. The effective intracellular resistivity is not uniform and has the average value R_{DF} (Ω -cm) in DF or R_{MF} (Ω -cm) in MF. The scaling resistivities in R_s are more accurately given by the parallel resistivities for extracellular (R_e Ω -cm) and intracellular current flow. In normal physiologic conditions, $R_e \gg R_{DF, MF}$, so Equation 2 is presented in terms of $R_{DF, MF}$. Resistivity depends inversely on the number of open-gap junction channels, the ionic strength of cytoplasm, and the radial distance between gap junctions (~fiber cell width). It is unlikely that all of these factors are exactly constant within either DF or MF. Nevertheless, the use of just two values of effective intracellular resistivity has proven to provide good fits to R_s data, and that is true for the data presented here.

RESULTS

Role of Cx50 in Regulation of Surface Cell Pressure

If the opening of gap junction hemichannels in the feedback loop that regulates positive surface cell pressure involves Cx50 hemichannels, then KO of Cx50 should break the feedback loop. Consistent with this reasoning, activation of TRPV4 with GSK1016790A (GSK) did not affect surface cell pressure in the Cx50 KO lens (Fig. 2A). Normally, TRPV4 is activated by a positive deflection in Δp . Figure 2A shows the response when GSK was used to pharmacologically activate TRPV4 in WT lenses. GSK exposure resulted in a negative change in Δp_i , which is the expected response to a positive deflection in Δp_i . Subsequently, Δp_i returned to zero over a period of approximately 2 hours, due to activation of TRPV1.²⁵ In Cx50 KO lenses, application of GSK did not cause a negative change in Δp_i , implying the connection between TRPV4 and the Na/K ATPase was broken. This is consistent with Cx50 providing the hemichannels responsible for release of ATP and activation of the subsequent steps.

In Figure 2B, a half-saturating concentration of the Na/K ATPase inhibitor strophanthidin was used to induce a positive deflection in Δp . A half-saturating concentration was used so the remaining active Na/K pumps could respond to activation of TRPV4 and restore the pressure to zero. When a saturating concentration of strophanthidin was used,²⁴ the positive deflection in Δp_i was larger and did not recover to zero. The recovery of Δp to zero in WT lenses (Fig. 2B) was shown to be due to activation of TRPV4 and stimulation of Na/K ATPase activity, as inhibition of TRPV4 blocked the recovery.²⁵ In Figure 2B, the recovery was also absent in the Cx50 KO lenses. Again, this is consistent with Cx50 providing the hemichannels responsible for release of ATP and activation of the subsequent steps.

The data shown in Figures 2A and 2B are consistent with Cx50 hemichannels being a step in the feedback loop connecting activation of TRPV4 to regulation of surface cell pressure at zero. Moreover, since the absence of Cx50 completely eliminates the response, there may be no contribution of other hemichannel-forming connexins or pannexins.

Lenses from Cx50 KO mice are noticeably smaller than WT lenses³⁴ (see below). We considered the possibility that elimination of Cx50 expression has structural or other indirect effects on lenses, in addition to reducing gap junction coupling conductance, that alter feedback regulation of surface cell pressure. To examine this possibility, mefloquine (Mfq) was employed to acutely block Cx50 channels/hemichannels in the WT lens. Mfq is a selective inhibitor of gap junction channels or hemichannels formed by Cx50 or Cx36. At the 10- μ M concentration used here, Mfq does not inhibit channels formed by Cx43 or Cx46.³⁵ In previous studies on intact lenses and isolated epithelial cells, the changes in gap junction coupling were consistent with Mfq inhibiting Cx50 channels but not Cx46.^{6,36}

The effects of Cx50 channel blockade by Mfq (Figs. 2C, 2D) were essentially identical to the effects of Cx50 knockout (Figs. 2A, 2B). The ability of Mfq to eliminate the surface cell pressure response of WT lenses to GSK and strophanthidin reinforces the argument that the connection between TRPV4 activation and surface cell pressure is severed by elimination of Cx50 channels.

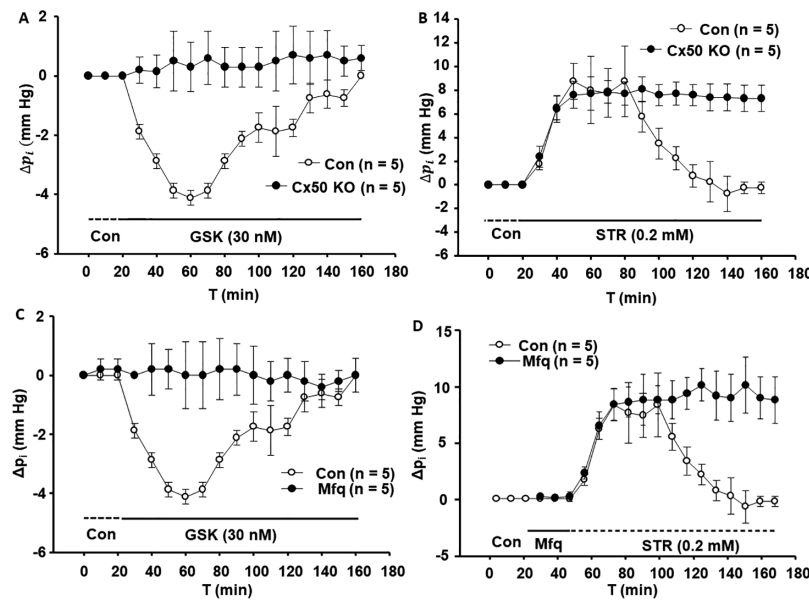


FIGURE 2. Surface cell pressure measurements in mouse lens show that elimination or blockade of Cx50 completely prevents TRPV4-dependent feedback responses. (A.) After establishing a stable baseline for 20 min, activation of TRPV4 by GSK caused a transient negative change in surface cell pressure. GSK did not change pressure in Cx50 KO lenses. (B) Lenses were subjected to partial inhibition of Na/K ATPase activity by strophanthidin (STR) in order to cause a positive deflection in surface cell pressure. After ~60 minutes in the presence of STR, the TRPV4-dependent feedback response in WT lenses gradually restored pressure to zero. Pressure was not restored in Cx50 KO lenses. (C) In WT lenses, blockade of Cx50 channels and hemichannels with the selective inhibitor Mfq (10 μ M) prevented the negative change in surface pressure caused by TRPV4 activation with GSK. (D) Also in WT lenses, Mfq prevented feedback reversal of the positive pressure deflection caused by STR.

Effect of Cx50 KO on the Radial Distribution of Gap Junctions and Intracellular Pressure

Knockout of Cx50 is expected to reduce the number of fiber cell gap junctions and thus increase the effective intracellular ionic resistivity (see Equation 2 and related text), as well as the effective intracellular hydraulic resistivity. Gap junction coupling was previously studied in Cx50 KO lenses from mice bred on the 129Sv genetic background³⁷ with results very similar to those shown here (Fig. 3A) for lenses from Cx50 KO mice of the C57 genetic background. Series resistance measured in WT and Cx50 KO lenses is presented as a function of the normalized distance from the lens center r/a , where r (cm) is the radial distance from the center and a (cm) is the lens radius. The series resistance represents the cumulative radial resistance of all the gap junctions between the lens surface and the location of the recorded data. The data were curve fit with Equation 2 to obtain average values of the effective resistivities of the central MF R_{MF} and peripheral DF R_{DF} . For comparison, Baldo et al.³⁷ reported the following values of resistivity in 129Sv lenses:

$$\begin{aligned} \text{WT 129Sv: } R_{DF} &= 3.5 \text{ K}\Omega\text{cm}, R_{MF} = 8.1 \text{ K}\Omega\text{cm}; \\ \text{Cx50 KO 129Sv: } R_{DF} &= 7.5 \text{ K}\Omega\text{cm}, R_{MF} = 23.3 \text{ K}\Omega\text{cm}. \end{aligned}$$

The effective intracellular resistivity is more than double in Cx50 KO lenses. However, the Cx50 KO lenses are also undersized, have faint optical distortion at their center, and deteriorate relatively quickly after dissection. This implies homozygous knockout of Cx50 could have indirect effects on Cx46 expression/gating. At 2 months old, the radius of the Cx50 KO lens was 0.101 ± 0.002 cm ($n = 8$) compared to 0.116 ± 0.003 cm ($n = 8$) in the WT. These dimensions are

essentially the same as those previously reported for Cx50 KO lenses bred on the mouse strain 129Sv.³⁷

Intracellular hydrostatic pressure in Cx50 KO lenses has not been previously measured. If Cx50 is in the feedback loop that responds to positive surface cell pressures, we reasoned that elimination of Cx50 might allow a positive uncontrolled drift in surface pressure. This appears to be the case (Fig. 3). When the data from Cx50 knockout lenses were fit with Equation 1, the projected value of surface pressure was $p_i(a) = 16$ mm Hg. In comparison, when the pressure data from WT lenses were curve fit with Equation 1, the projected value of surface pressure was $p_i(a) = 0$ mm Hg, as it was in all previous measurements of pressure in WT lenses from mice or other species. These data are consistent with the hypothesis that Cx50 hemichannels are in the feedback loop for regulation of positive surface cell pressures.

In Cx50 KO lenses relative to WT, there is an increase in surface intracellular pressure, but there is also a much larger increase in hydrostatic pressure in central fiber cells. The increase in the center to surface pressure gradient is consistent with the large increase in the effective intracellular resistivity of MF, R_{MF} , seen in Figure 2. The MF pressure gradient in Cx50 KO lenses is a factor of 1.8 times greater than that in WT lenses. The relative increase in R_{MF} in Cx50 KO versus WT lenses is a factor of 2.4. If intracellular ionic strength and water flow had remained the same in Cx50 KO and WT lenses, the increases relative to control in the pressure gradient and resistivity should have been almost the same.³ However, the measured increase relative to control in resistivity is greater than the increase relative to control in pressure, suggesting a possible reduction in fluid transport or ionic strength of the cytoplasm in the KO lenses. This is not surprising given the tendency of the Cx50 KO lenses to show signs of deterioration.

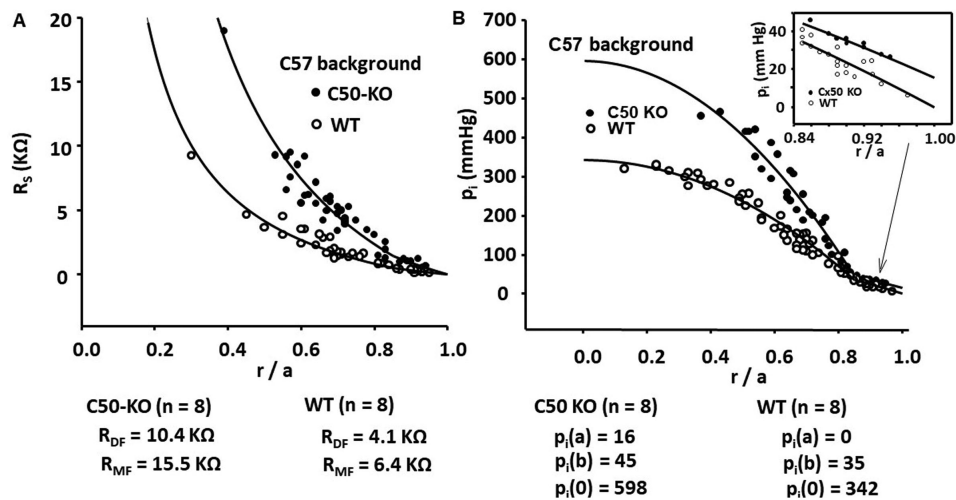


FIGURE 3. The radial distribution of resistance and intracellular hydrostatic pressure is different in WT versus Cx50 KO lenses. (A) The high-frequency input resistance (R_S) of WT (open circles) and Cx50 KO (filled circles) lenses graphed as a function of normalized distance from the lens center ($r/a = 0$) to the surface ($r/a = 1.0$). The magnitude of R_S represents the cumulative radial resistance of all gap junctions between the surface of the lens and the point of recording. The solid line was fitted to the data by calculating R_S from Equation 2 (see Methods) using the indicated values of effective intracellular resistivity of DF R_{DF} and MF R_{MF} in WT and KO lens. Note that DF change to MF at $r/a = 0.85$. (B) The intracellular hydrostatic pressure gradients in WT and Cx50 KO lenses. Intracellular pressure ($p_i(r)$) is generated by water flow velocity times the effective intracellular hydraulic resistivity, which depends inversely on the number of open gap junction channels, as does R_{DF} and R_{MF} . The solid line indicates $p_i(r)$ fitted to the data using Equation 1 and the indicated values at the lens center, $p_i(0)$ at the differentiating to mature fiber (DF to MF) transition $p_i(b)$, and at the lens surface $p_i(a)$. The inset shows part of the same data drawn on an expanded scale to illustrate the difference in DF pressures between WT and Cx50 KO lenses. The calculated smooth curves are essentially the mean value of the data, and the scatter of the data about these curves provides a visual estimate of the standard deviation.

Two Pathways Connect TRPV1 Activation to Regulation of Surface Pressure

Sellitto et al.²⁴ provided convincing evidence that chronic activation of Akt through knockout of PTEN led to reduced Na/K ATPase activity, which positively increased surface intracellular pressure. When Gao et al.²⁵ identified TRPV1 as the sensor for negative deflections in surface intracellular pressure and that TRPV1 activation led to Akt activation, they assumed that restoration of negative pressure to 0 mm Hg was due to reduced Na/K ATPase activity. However, Shahdullah et al.^{32,33} provided convincing evidence that the short-term (20-minute) response to a negative deflection in surface intracellular pressure was due to activation of NKCC and not inhibition of Na/K ATPase activity. Figure 4 appears to resolve this contradiction.

Figure 4A shows the response of a WT lens to a negative deflection in lens surface cell intracellular hydrostatic pressure.³³ The pressure can be made to go negative either by increasing the external osmolarity, as in Figure 4A, or by reducing intracellular osmolarity through pharmacologic activation of TRPV4,²⁵ which causes an increase in Na/K ATPase activity.^{26,27} In either case, the pressure requires approximately 20 minutes to reach its maximum negative value, and then it recovers back to 0 mm Hg over a period of approximately 2 hours. The negative pressure is sensed by TRPV1, which stimulates PI3K/Akt activity.^{25,33} The short-term effect of increased PI3K/Akt activity is to increase NKCC activity,³³ which increases intracellular osmolarity to restore intracellular pressure to 0 mm Hg (Fig. 4A).

When NKCC is blocked with a saturating concentration of bumetanide (Fig. 4B), the short-term response to a nega-

tive pressure is also blocked, but there is a delayed, long-term (>200-minute) response that restores pressure to 0 mm Hg. We have evidence that the short-term response mechanism involves NKCC activation,^{32,33} and our working hypothesis is that the long-term response mechanism involves reduced Na/K ATPase activity.²⁴ If this is so, reduction in Na/K ATPase activity appears to be a backup process that takes effect when NKCC cannot restore pressure to zero.

If the long-term response mechanism involves TRPV1 sensing the negative pressure and causing Akt activation, then knockout of TRPV1 or blockade of Akt should eliminate the response. An alternative possibility is the long-term response is simply due to nonspecific transmembrane electrodiffusion leading to an intracellular osmotic change that balances out the need for intracellular pressure. In studies to test these possibilities, we found the long-term response requires the presence of TRPV1, since the response is lost in the TRPV1 KO lenses (Fig. 5A). Moreover, both Figures 5A and 5B suggest that nonspecific transmembrane electrodiffusion will not generate an osmotic change that balances the intracellular pressure. Figure 5B supports the idea that the long-term response is subject to signaling by PI3K/Akt,²⁴ since the response is lost when Akt is blocked with the specific inhibitor Akti in WT lenses. It is important to note that in both these studies, NKCC is available but not activated to provide the short-term response, suggesting both short-term and long-term responses are initiated by TRPV1 activation and signaling for both responses goes through PI3K/Akt. Our current hypothesis for feedback control of surface intracellular pressure is shown in Figure 7 of the Discussion.

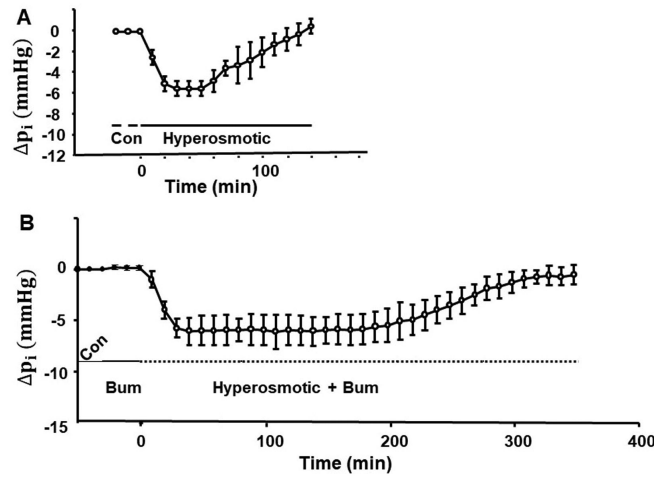


FIGURE 4. Lens surface cell pressure changes induced by hyperosmotic solution (Tyrode + 20 mOsm mannitol). **(A)** In WT lenses, hyperosmotic solution caused a decrease in pressure of approximately 6 mm Hg that lasted approximately 20 minutes, and then the pressure returned to 0 mm Hg over a period of approximately 2 hours (data from Shahidullah et al.³³). **(B)** In the presence of the NKCC inhibitor bumetamide (Bum, 10 μ M), hyperosmotic solution caused a decrease in pressure of approximately 8 mm Hg over a period of approximately 20 minutes, but the decrease persisted for ~3 hours. After that, pressure gradually returned to 0 mm Hg over a period of approximately 2 more hours.

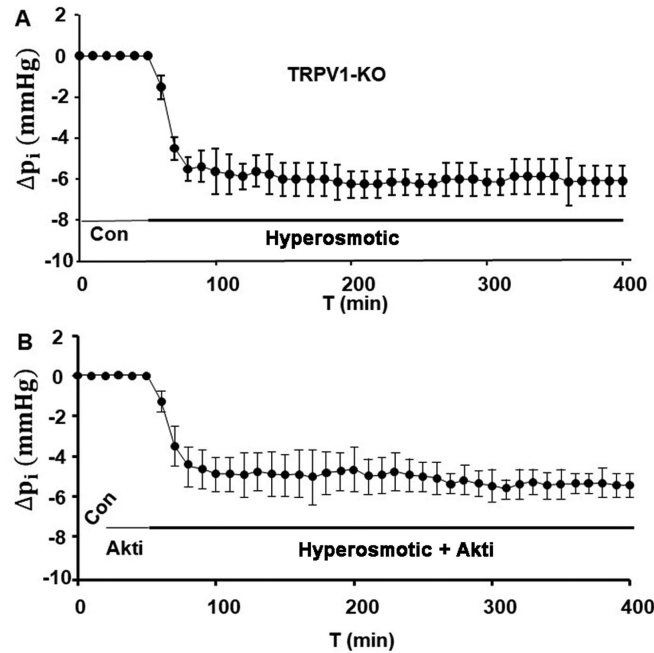


FIGURE 5. The long-term pressure recovery response after a negative pressure deflection is abolished by elimination of TRPV1 or inhibition of PI3K/Akt signaling. **(A)** The negative change in surface cell pressure caused by hyperosmotic solution (Tyrode + 20 mOsm mannitol) did not recover in TRPV1 KO lenses. **(B)** There was also no recovery in the presence the Akt inhibitor Akti (10 μ M) in WT lenses.

Effect of TRPV1 KO on the Radial Distribution of Gap Junctions and Intracellular Pressure

There was no a priori reason to expect knockout of TRPV1 would affect gap junction coupling of fiber cells, and it was evident that the series resistances for TRPV1 KO and WT lenses are almost identical (Fig. 6A). The results indicate

that TRPV1 KO does not affect gap junction coupling, a finding consistent with the normal size and transparency of the lenses.

Since TRPV1 protects the lens against negative deflections in surface cell hydrostatic pressure, we thought knockout of TRPV1 might cause a negative drift in surface pressure. However, the WT and TRPV1 pressure gradients shown

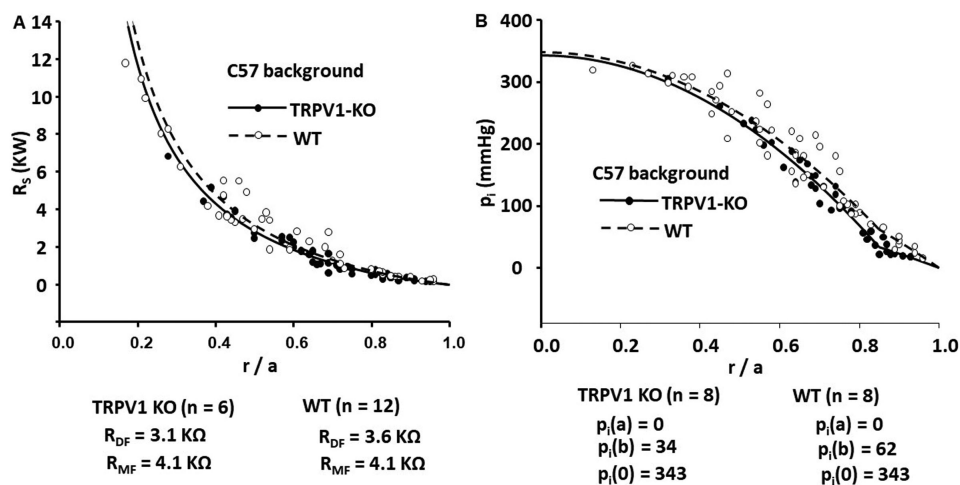


FIGURE 6. The radial distribution of resistance and intracellular hydrostatic pressure is similar in WT and TRPV1 KO lenses. **(A)** The high-frequency input resistance (R_s) of WT (*open circles*) and TRPV1 KO (*filled circles*) lenses graphed as a function of normalized distance from the lens center ($r/a = 0$) to the surface ($r/a = 1.0$). The magnitude of R_s represents the cumulative radial resistance of all gap junctions between the surface of the lens and the point of recording. The *solid line* was fitted to the data by calculating R_s from Equation 2 (see Methods) using the indicated values of effective intracellular resistivity of DF R_{DF} and MF R_{MF} in WT and TRPV1 KO lenses. Note that DF change to MF at $r/a = 0.85$. There appears to be no detectable effect of TRPV1 KO on gap junction coupling. **(B)** The intracellular hydrostatic pressure gradients in WT and TRPV1 KO lenses. The *solid line* indicates the pressure ($p_i(r)$) fitted to the data using Equation 1 and the indicated values at the lens center $p_i(0)$, at the DF to MF transition $p_i(b)$, and at the lens surface $p_i(a)$. The calculated smooth curves are essentially the mean value of the data, and the scatter of the data about these curves provides a visual estimate of the standard deviation.

in Figure 6B are very similar and suggest there is no significant effect of TRPV1 knockout on surface pressure. The curve fit to the data determines three parameters, the central pressure ($p_i(0)$ $r/a = 0$), the pressure at the DF to MF transition ($p_i(b)$ $r/a = 0.85$), and the surface pressure ($p_i(a)$ $r/a = 1$). The surface pressure is 0 mm Hg (the best fit projects $p_i(a) \approx 10^{-9}$ mm Hg) in both types of lenses. The pressure gradient in the DF of the TRPV1 KO lenses does appear to be somewhat less than that in the DF of WT lenses ($p_i(b) = 34$ mm Hg in KO versus 62 mm Hg in WT), but the difference might just be normal biological variation. If one looks at the WT pressure gradient shown in Figure 3B, it is almost identical to that in the TRPV1 KO shown in Figure 6B. We conclude there is no detectable effect of TRPV1 KO on lens intracellular pressure, at least within the accuracy of our measurement.

DISCUSSION

The results reported here add two critical pieces of new information. First, the consequences of Cx50 elimination on pressure responses make it evident that Cx50 is essential for the feedback path that connects between TRPV4 and surface cell pressure. The simplest hypothesis consistent with all the data is that Cx50 forms the hemichannels that are opened when TRPV4 is activated by a positive deflection in surface cell pressure. Earlier studies by Shahidullah et al.^{26,27} indicated open hemichannels allow ATP release and P2Y activation, leading to Src kinase activation and ultimately increased Na/K ATPase activity. The increase in Na/K ATPase activity reduces intracellular osmolarity and decreases pressure back to zero.²⁵ Based on the ability of probenecid to partially inhibit TRPV4-dependent ATP release and propidium uptake responses in porcine lens, it was suggested previously that pannexin channels as well as connexins contribute to the hemichannel opening response.^{26,27} In contrast, the fact that Mfj and Cx50

knockout were found to completely prevent the pressure responses in mouse lens suggests there is no significant functional contribution of pannexins or other connexins.

The second major addition from the current study is the finding of a long-term pressure recovery response that is able to correct a negative surface cell pressure even when NKCC is inhibited. The response is TRPV1 dependent as well as Akt dependent. Our working hypothesis is that the long-term response involves delayed inhibition of Na/K ATPase activity. There is ample evidence that Akt signaling influences lens Na/K ATPase activity. Taken together, our results suggest that in instances of small, brief negative excursion in surface cell pressure, only NKCC stimulation is recruited, but if the problem persists, decreased Na/K ATPase activity comes into play. Either response has the effect of increasing intracellular osmolarity and increases pressure back to zero.

Accumulation of myoinositol has previously been shown to play a role in lens osmoregulation, and the Na-myoinositol transporter is upregulated by prolonged hyperosmotic stimuli.³⁸ However, myoinositol was not added to the bathing medium in these experiments. We cannot rule out the role of Na-myoinositol transporter on intracellular osmolarity in vivo. Further study is needed to determine the effect of TRPV1 or Akt on Na-myoinositol transport.

Roles of Cx50 in the Lens

Studies of Cx50 keep revealing new roles for this protein. It was the first connexin identified in lens fiber cell gap junctions,^{39,40} where it was assumed to be responsible for electrical and metabolic communication between fiber cells. However, Cx46 was also identified as a lens fiber cell gap junction protein,⁴¹ so the following question arose: why does the lens need two different connexins to mediate communication between fibers? Mathias et al.¹⁴ reported an abrupt reduction in gap junction coupling conductance at the DF to MF transition, where connexins are subjected to C-terminal

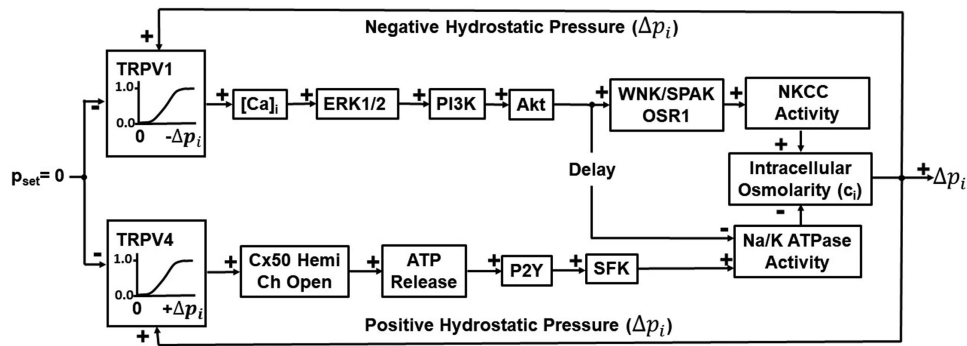


FIGURE 7. An updated feedback control system for hydrostatic pressure in surface cells of the lens. An *arrow* with a + sign means an increase or decrease of the upstream event causes an increase or decrease in the downstream event; an arrow with a - sign means an increase or decrease of the upstream event causes a decrease or increase in the downstream event. A perturbation in surface cell pressure Δp_i could be either positive or negative. Positive Δp_i is sensed by TRPV4, and signaling is initiated to increase Na/K ATPase activity, reduce osmolarity, and reduce pressure back to zero. Negative Δp_i is sensed by TRPV1 and signaling is initiated to first increase activity of NKCC, which should increase osmolarity and pressure. If NKCC does not restore pressure to 0 mm Hg, after a delay, Akt signaling initiates a decrease in Na/K ATPase activity, which increases osmolarity and pressure back to 0 mm Hg.

cleavage. Subsequent studies¹⁵ suggested the reduction in coupling conductance at the DF to MF transition involved the closure of Cx50 channels in the MF. Other studies on Cx46 heterozygous and homozygous knockout lenses⁴² and Cx50 heterozygous knockout lenses³⁷ also suggested that most open gap junction channels in MF are composed of Cx46. Thus, Cx46 may actually be the protein responsible for electrical and metabolic coupling of all fiber cells, and Cx50 has other roles.

Knockout of Cx50 revealed that it was involved in regulation of lens growth during development, as the knockout lenses and eyeballs were undersized.^{34,43,44} We also found that the presence of Cx50 channels was necessary for pH-induced gating of Cx46 channels, implying cooperative gating between neighboring Cx50 and Cx46 channels in the DF.^{36,37} The physiologic role of cooperative gating has not been demonstrated, but there is a poles-to-equator gradient in the number of open gap junction channels in the DF,¹⁷ and Cx50 may be involved in maintaining the relatively high coupling of equatorial fibers and very low coupling of polar fibers.⁷ More recently, Hu et al.⁴⁵ found Cx50 has a role in cell-to-cell adhesion (independent of channel formation) and promoted lens cell differentiation. Here, we have shown Cx50 has a role in the regulation of surface cell hydrostatic pressure in the lens.

The TRPV1-Mediated Pathway

The scheme in **Figure 7** explains how a negative pressure is sensed by TRPV1, which then activates PI3K to phosphorylate Akt and stimulate transport by NKCC. We show that under normal circumstances, NKCC can restore pressure to zero within a couple of hours. This transporter, which is electroneutral and thus independent of membrane potential, is energetically coupled to three ion gradients across the plasma membrane, Na^+ , K^+ , and Cl^- . NKCC is a relatively fast transport mechanism, but it has limited authority because its continued operation brings it closer to equilibrium. The driving force for NKCC is described by the following equation:

$$\frac{\Delta G}{F} = 2E_{\text{Cl}} - E_{\text{K}} - E_{\text{Na}}$$

ΔG (Joules/mole) is the change in free energy per mole of solute transported and F is Faraday's constant. $\Delta G/F$ has the units volts, and it depends on the Nernst potentials of the three transported ions: E_{Cl} , E_{K} , and E_{Na} . At equilibrium, $\Delta G = 0$ and the cotransporter no longer has the ability to assist in osmoregulation. Based on estimates of Nernst potentials in the normal lens epithelium, $\Delta G/F$ for NKCC is around -70 mV, which is not very far from equilibrium, whereas the Na/K ATPase is approximately -270 mV from equilibrium.

If Na/K ATPase inhibition indeed accounts for the delayed, long-term pressure response, the findings suggest TRPV1-dependent, Akt-mediated inhibition of Na/K pump activity is much slower than activation of NKCC. We have insufficient evidence to speculate on a mechanistic explanation for why this path is slow to be activated. The important point to keep in mind is that Na/K pump inhibition has tremendous authority, because without Na/K pump activity, any cell would swell until it ruptures. It is the only mechanism capable of harnessing the energy of ATP hydrolysis to maintain ion/osmotic homeostasis.

It is worth considering PTEN knockout lenses. Here, TRPV4-initiated stimulation of Na/K pump activity is probably induced by the positive surface cell pressure, but it appears Akt-mediated inhibition of pump activity dominates. However, when Akt was inhibited in PTEN KO lenses, surface cell pressure rapidly returned to zero,²⁴ probably due to the TRPV4 path. In the PTEN knockout lenses, NKCC probably shifts ions to the point where its driving force approaches equilibrium, and without inhibition of the Na/K pumps, the lenses would not have ruptured.

Unanswered Questions

We are left with several unanswered questions, both specific and general. There are specific questions regarding several steps that still need to be elucidated in the signaling mechanism (**Fig. 7**). How do two different calcium channels, TRPV1 and TRPV4, exert such divergent calcium signaling-dependent effects on cell function? How does TRPV4 activation cause hemichannels to open? Not only are there steps missing in the pathways we have identified, but there may be other pathways for regulation of pressure. Here

we focus on surface pressure regulation, but there is also the center-to-surface pressure gradient, which also may be regulated. Chen et al.⁴⁶ showed that the center-to-surface pressure gradient in mouse lenses could be increased or decreased respectively by contraction or relaxation of the ciliary muscle. They further showed the increase was mediated by TRPV1 and the decrease by TRPV4. These results suggest the TRPV1/4-mediated pathways could be significantly more complex than shown in Figure 7. Moreover, there may be other regulatory pathways that are independent of TRPV1/4. For example, when the TRPV4 pathway was eliminated, the surface intracellular pressure drifted positive (Fig. 3B) as expected since the TRPV4 pathway appears to protect against positive surface pressure drift. However, when the TRPV1 pathway was eliminated, the surface intracellular pressure did not change from 0 mm Hg (Fig. 6B). We thought there would be negative surface pressure drift, since the TRPV1 pathway appears to protect against negative surface pressure drift, but this did not happen. This suggests negative drift may be prevented by yet another pathway, a very long-term pathway that is independent of TRPV1. This pathway was not seen in the 6-hour experiments shown in Figures 5 and 6, but TRPV1 KO is a lifetime change and could elicit compensatory responses.

Finally, there is the general question of why the lens hydrostatic pressure is regulated. We know from recent studies that the lens circulation is required to maintain an intracellular center-to-surface gradient in protein concentration.⁴⁷ The free energy of biological solutions depends on their osmolarity and hydrostatic pressure, so the osmolarity generated by the protein gradient is directly coupled to the lens pressure gradient. Having a higher protein content at the lens center is essential for lens optics because it gives rise to a gradient in refractive index that reduces spherical aberration. Although the lens circulation has previously been thought of in terms of its physiologic role, the regulatory mechanisms that control the circulation may also be critical to lens being a living optical element.

Acknowledgments

Supported by National Institutes of Health Grants EY013163 and EY026911 to TWW and EY009532 to NAD.

Disclosure: **N.A. Delamere**, None; **M. Shahidullah**, None; **R.T. Mathias**, None; **J. Gao**, None; **X. Sun**, None; **C. Sellitto**, None; **T.W. White**, None

References

- Delamere NA, Tamiya S. Expression, regulation and function of Na,K-ATPase in the lens. *Prog Retin Eye Res.* 2004;23:593–615.
- Candia OA, Zamudio AC. Regional distribution of the Na(+) and K(+) currents around the crystalline lens of rabbit. *Am J Physiol Cell Physiol.* 2002;282:C252–C262.
- Gao J, Sun X, Moore LC, White TW, Brink PR, Mathias RT. Lens intracellular hydrostatic pressure is generated by the circulation of sodium and modulated by gap junction coupling. *J Gen Physiol.* 2011;137:507–520.
- Beyer EC, Paul DL, Goodenough DA. Connexin43: a protein from rat heart homologous to a gap junction protein from liver. *J Cell Biol.* 1987;105:2621–2629.
- Rae JL, Bartling C, Rae J, Mathias RT. Dye transfer between cells of the lens. *J Membr Biol.* 1996;150:89–103.

- White TW, Gao J, Li L, Sellitto C, Srinivas M. Optimal lens epithelial cell proliferation is dependent on the connexin isoform providing gap junctional coupling. *Invest Ophthalmol Vis Sci.* 2007;48:5630–5637.
- Boswell BA, Le AC, Musil LS. Upregulation and maintenance of gap junctional communication in lens cells. *Exp Eye Res.* 2009;88:919–927.
- Delamere NA, Dean WL. Distribution of lens sodium-potassium-adenosine triphosphatase. *Invest Ophthalmol Vis Sci.* 1993;34:2159–2163.
- Mathias RT, Rae JL, Ebihara L, McCarthy RT. The localization of transport properties in the frog lens. *Biophys J.* 1985;48:423–434.
- Webb KF, Donaldson PJ. Differentiation-dependent changes in the membrane properties of fiber cells isolated from the rat lens. *Am J Physiol Cell Physiol.* 2008;294:C1133–C1145.
- Tong JJ, Acharya P, Ebihara L. Calcium-activated chloride channels in newly differentiating mouse lens fiber cells and their role in volume regulation. *Invest Ophthalmol Vis Sci.* 2019;60:1621–1629.
- Kistler J, Christie D, Bullivant S. Homologies between gap junction proteins in lens, heart and liver. *Nature.* 1988;331:721–723.
- Mathias RT, White TW, Gong X. Lens gap junctions in growth, differentiation, and homeostasis. *Physiol Rev.* 2010;90:179–206.
- Mathias RT, Rae JL, Eisenberg RS. The lens as a nonuniform spherical syncytium. *Biophys J.* 1981;34:61–83.
- DeRosa AM, Mui R, Srinivas M, White TW. Functional characterization of a naturally occurring Cx50 truncation. *Invest Ophthalmol Vis Sci.* 2006;47:4474–4481.
- Piatigorsky J. Lens differentiation in vertebrates: a review of cellular and molecular features. *Differentiation.* 1981;19:134–153.
- Baldo GJ, Mathias RT. Spatial variations in membrane properties in the intact rat lens. *Biophys J.* 1992;63:518–529.
- Candia OA, Zamudio AC. Regional distribution of the Na(+) and K(+) currents around the crystalline lens of rabbit. *Am J Physiol Cell Physiol.* 2002;282:C252–C262.
- Gao J, Sun X, Yatsula V, Wymore RS, Mathias RT. Isoform-specific function and distribution of Na/K pumps in the frog lens epithelium. *J Membr Biol.* 2000;178:89–101.
- Vaghefi E, Pontre BP, Jacobs MD, Donaldson PJ. Visualizing ocular lens fluid dynamics using MRI: manipulation of steady state water content and water fluxes. *Am J Physiol Regul Integr Comp Physiol.* 2011;301:R335–R342.
- Candia OA, Mathias R, Gerometta R. Fluid circulation determined in the isolated bovine lens. *Invest Ophthalmol Vis Sci.* 2012;53:7087–7096.
- Gao J, Wang H, Sun X, et al. The effects of age on lens transport. *Invest Ophthalmol Vis Sci.* 2013;54:7174–7187.
- Gao J, Sun X, Moore LC, White TW, Brink PR, Mathias RT. The effect of size and species on lens intracellular hydrostatic pressure. *Invest Ophthalmol Vis Sci.* 2013;54:183–192.
- Sellitto C, Li L, Gao J, et al. AKT activation promotes PTEN hamartoma tumor syndrome-associated cataract development. *J Clin Invest.* 2013;123:5401–5409.
- Gao J, Sun X, White TW, Delamere NA, Mathias RT. Feedback regulation of intracellular hydrostatic pressure in surface cells of the lens. *Biophys J.* 2015;109:1830–1839.
- Shahidullah M, Mandal A, Delamere NA. TRPV4 in porcine lens epithelium regulates hemichannel-mediated ATP release and Na-K-ATPase activity. *Am J Physiol Cell Physiol.* 2012;302:C1751–C1761.
- Shahidullah M, Mandal A, Delamere NA. Hyposmotic stress causes ATP release and stimulates Na,K-ATPase activity in porcine lens. *J Cell Physiol.* 2012;227:1428–1437.

28. White TW, Deans MR, O'Brien J, et al. Functional characteristics of skate connexin35, a member of the gamma subfamily of connexins expressed in the vertebrate retina. *Eur J Neurosci.* 1999;11:1883–1890.
29. Hoang QV, Qian H, Ripps H. Functional analysis of hemichannels and gap-junctional channels formed by connexins 43 and 46. *Mol Vis.* 2010;16:1343–1352.
30. Srinivas M, Jannace TF, Cocozzelli AG, et al. Connexin43 mutations linked to skin disease have augmented hemichannel activity. *Sci Rep.* 2019;9:19.
31. Srinivas M, Kronengold J, Bukauskas FF, Bargiello TA, Verselis VK. Correlative studies of gating in Cx46 and Cx50 hemichannels and gap junction channels. *Biophys J.* 2005;88:1725–1739.
32. Shahidullah M, Mandal A, Delamere NA. Activation of TRPV1 channels leads to stimulation of NKCC1 cotransport in the lens. *Am J Physiol Cell Physiol.* 2018;315:C793–C802.
33. Shahidullah M, Manda A, Mathias RT, et al. TRPV1 activation stimulates NKCC1 and increases hydrostatic pressure in mouse lens. *Am J Physiol Cell Physiol.* 2020;318:C969–C980.
34. White TW, Goodenough DA, Paul DL. Targeted ablation of connexin50 in mice results in microphthalmia and zonular pulverulent cataracts. *J Cell Biol.* 1998;143:815–825.
35. Cruikshank SJ, Hopperstad M, Younger M, Connors BW, Spray BC, Srinivas M. Potent block of Cx36 and Cx50 gap junction channels by mefloquine. *Proc Natl Acad Sci USA.* 2001;101:12364–12369.
36. Martinez-Wittinghan FJ, Srinivas M, Sellitto C, White TW, Mathias RT. Mefloquine effects on the lens suggest cooperative gating of gap junction channels. *J Membr Biol.* 2006;211:163–171.
37. Baldo GJ, Gong X, Martinez-Wittinghan FJ, Kumar NM, Gilula NB, Mathias RT. Gap junctional coupling in lenses from alpha(8) connexin knockout mice. *J Gen Physiol.* 2001;118:447–456.
38. Cammarata PR, Xu GT, Huang L, Zhou C, Martin M. Inducible expression of Na⁺/myoinositol cotransport mRNA in the anterior epithelium of bovine lens: affiliation with hypertonicity and cell proliferation. *Exp Eye Res.* 1997;64:745–747.
39. Kistler J, Bullivant S. Dissociation of lens fibre gap junctions releases MP70. *J Cell Sci.* 1988;91:415–421.
40. White TW, Bruzzone R, Goodenough DA, Paul DL. Mouse Cx50, a functional member of the connexin family of gap junction proteins, is the lens fiber protein MP70. *Mol Biol Cell.* 1992;3:711–720.
41. Paul DL, Ebihara L, Takemoto LJ, Swenson KI, Goodenough DA. Connexin46, a novel lens gap junction protein, induces voltage-gated currents in nonjunctional plasma membrane of *Xenopus* oocytes. *J. Cell Biol.* 1991;115:1077–1089.
42. Gong X, Baldo GJ, Kumar NM, Gilula NB, Mathias RT. Gap junctional coupling in lenses lacking alpha3 connexin. *Proc Natl Acad Sci USA.* 1998;95:15303–15308.
43. Rong P, Wang X, Niesman I, et al. Disruption of Gja8 (alpha8 connexin) in mice leads to microphthalmia associated with retardation of lens growth and lens fiber maturation. *Development.* 2002;129:167–174.
44. Sellitto C, Li L, White TW. Connexin50 is essential for normal postnatal lens cell proliferation. *Invest Ophthalmol Vis Sci.* 2004;45:3196–3202.
45. Hu Z, Shi W, Riquelme MA, et al. Connexin 50 functions as an adhesive molecule and promotes lens cell differentiation. *Sci Rep.* 2017;7:5298.
46. Chen Y, Gao J, Li L, Sellitto C, Donaldson PJ, White TW. The ciliary muscle and zonules of Zinn modulate lens intracellular hydrostatic pressure through transient receptor potential vanilloid channels. *Invest Ophthalmol Vis Sci.* 2019;60:4416–4424.
47. Vaghefi E, Kim A, Donaldson PJ. Active maintenance of the gradient of refractive index is required to sustain the optical properties of the lens. *Invest Ophthalmol Vis Sci.* 2015;56:7195–7208.